1-1-2009

A family of pseudo-Anosov maps

Mark Demers
Fairfield University, mdemers@fairfield.edu

Marciej P. Wojtkowski

Published Citation

Mark Demers and Maciej P. Wojtkowski, "A family of pseudo-Anosov maps," Nonlinearity, 22:7 (2009), 1743-1760.

A family of pseudo-Anosov maps

Mark F. Demers* Maciej P. Wojtkowski†

June 11, 2009

Abstract

We study a family of area-preserving maps of the 2-torus and show that they are pseudo-Anosov. We present a method to construct finite Markov partitions for this family which utilizes their common symmetries. Through these partitions we show explicitly that each map is a tower over a first return map, intimately linked to a toral automorphism. This enables us to calculate directly some dimensional characteristics of the dynamics.

1 Introduction

Let us consider the following class of area preserving maps of the torus $H : \mathbb{T}^2 \to \mathbb{T}^2$

$$H \begin{bmatrix} x \\ y \end{bmatrix} = \begin{bmatrix} x + y + g(x) \\ y + g(x) \end{bmatrix}$$

where (x, y) are *mod* 1 coordinates on $\mathbb{T}^2$, and $g(x)$ is a continuous periodic function with period 1.

This map can also be considered on the cylinder $\mathbb{T}^1 \times \mathbb{R}$. If the map has an invariant curve of the form $y = \varphi(x)$ for some periodic function $\varphi(x)$ then by necessity $\int_0^1 g(x)dx = 0$. For $g(x) = K \sin 2\pi x$ we obtain the Chirikov-Taylor standard map. For $g(x) = K(|x| - \frac{1}{4}), -\frac{1}{2} \leq x \leq \frac{1}{2}$ we get its piecewise linear version studied in [W1, W2, Bu]. In particular it was shown in [W1] that for $K = 2$, i.e., for $g(x) = 2|x| - \frac{1}{2}$, outside of an invariant parallelogram the map is nonuniformly hyperbolic (and mixing [LW]). The stable and unstable leaves are piecewise linear; however, they are well-defined only almost everywhere and their direction varies only measurably. Cerbelli and Giona [CG] discovered that adding an upward shift of $\frac{1}{2}$, i.e., $g(x) = 2|x|$ for $-\frac{1}{2} \leq x \leq \frac{1}{2}$, makes the map hyperbolic everywhere, and moreover

*Department of Mathematics and Computer Science, Fairfield University, Fairfield CT 06824, USA. mdemers@fairfield.edu.

†Department of Mathematics and Informatics, University of Warmia and Mazury, ul Zolnierska 14, 10-561 Olsztyn, Poland. wojtkowski@matman.uwm.edu.pl.

2000 Mathematics Subject Classification: 37E30, 37D35, 37C45.

The authors would like to thank MSRI, Berkeley, where this project was started and ESI, Vienna, where much progress was made. MD was supported in part by NSF grant DMS-0801139. MPW was partially supported by the Polish Ministry of Science and Higher Education grant N201 270535.

the directions of stable and unstable leaves become piecewise constant. For this choice of g, MacKay [M] provided an extensive mathematical analysis of the map, showing in particular that the map is pseudo-Anosov, and constructing for it a geometric Markov partition.

In this paper we include the Cerbelli-Giona map in an infinite discrete family $H_k : \mathbb{T}^2 \to \mathbb{T}^2$, $k \in \mathbb{Z}$, $|k| \geq 2$, defined by

$$H_k \begin{bmatrix} x \\ y \end{bmatrix} = \begin{bmatrix} (k-1)x + y + g_k(x) \\ (k-2)x + y + g_k(x) \end{bmatrix}$$

where $g_k(x)$ is a continuous periodic function with period 1, $g_k(x) = k|x|$, $-\frac{1}{2} \leq x \leq \frac{1}{2}$.

We show that the maps share many properties and construct a symmetric Markov partition for each member of the family (Sections 2 and 3). In Section 4, we show explicitly how the maps can be viewed as towers over Markov return maps, which in turn generate Markov processes identical to those induced by a corresponding family of toral automorphisms. This structure allows us to calculate some dimensional characteristics of the dynamics for all values of k in a simpler way compared with the calculations in [M] for $k = 2$. Namely, we consider the level sets of the positive Lyapunov exponent. Their Hausdorff dimension is an analytic function for which we obtain a fairly simple description. Since our system is piecewise linear and it has a Markov partition, we can use for that purpose the classical theorem of Billingsley [B].

2 The family and its symmetries

There is another way to represent the map H. Let us make the following change of variables $u = x - y, v = x$. In these variables the map H becomes

$$T \begin{bmatrix} u \\ v \end{bmatrix} = \begin{bmatrix} v \\ -u + G(v) \end{bmatrix}$$

with $G(v) = 2v + g(v)$. It is straightforward to check that T defines an area-preserving homeomorphism of the torus for any circle map G, $G(v) = kv + g(v)$ for an integer k and a periodic function $g(v)$.

Let us consider the involution $S(u, v) = (v, u)$. The reflection S satisfies

$$S \circ T = T^{-1} \circ S,$$

i.e., the map T is reversible with respect to S. The advantage of this representation of the map comes from the fact that this symmetry is "skewed" in the original coordinates, and hence less visible.

We also introduce another involution $C(u, v) = \left(\frac{1}{2} - u, \frac{1}{2} - v\right)$. The map C is the rotation by π around the point $\left(\frac{1}{4}, \frac{1}{4}\right)$, as viewed on the plane. On the torus the map C has four fixed points at $\left(\pm\frac{1}{4}, \pm\frac{1}{4}\right)$, and hence it can be considered equally well as the rotation by π around any of them. The map T has additional symmetry with respect to C, namely

$$C \circ T = T \circ C, \tag{1}$$

provided that the function G satisfies

$$G(\tfrac{1}{2} - v) = -G(v), \quad mod\ 1. \tag{2}$$

2.1 A 1-parameter family of maps

The family of maps $T = T_k$ we shall study in this paper is defined by choosing $G_k(v) = kv + g(v)$ where k is allowed to assume any integer value $k, |k| \geq 2$, and $g(v)$ is the periodic function $g(v) = k|v|$, $-\frac{1}{2} \leq v \leq \frac{1}{2}$, i.e,

$$G(v) = G_k(v) = \begin{cases} 0 & \text{for } -\frac{1}{2} \leq v \leq 0 \\ 2kv & \text{for } 0 \leq v \leq \frac{1}{2} \end{cases} .$$

Such piecewise linear maps for $k = 0, \pm 1$ were studied in [CW]. For $k = 2$ we get the Cerbelli-Giona map, [CG]. Our functions G_k do satisfy (2) so that the maps T_k enjoy the self-symmetry given by (1). In (x, y) coordinates, the mappings T_k are equal to the mappings H_k from the introduction.

We use the square $[-.5, .5] \times [-.5, .5]$ as our fundamental domain for $\mathbb{T}^2$ and partition it into quadrants using the coordinate axes. We use the numbering of quadrants $Q4, Q1, Q2, Q3$ starting with the positive quadrant and progressing **clockwise** about the origin. The reason for this numbering scheme will become clear once we define our Markov partitions.

For $v < 0$, the map T is clockwise rotation by $\pi/2$ about the origin, i.e., $T(u, v) = (v, -u)$. So $Q1$ and $Q2$ are mapped into $Q2$ and $Q3$ respectively. Moreover $Q1$ is mapped under T^2 into $Q3$ so that T^2 there corresponds to clockwise rotation by π.

For $v > 0$, the map $T = T_k$ is the same clockwise rotation by $\pi/2$ followed by a vertical shear

$$T_k \begin{bmatrix} u \\ v \end{bmatrix} = A_k \begin{bmatrix} u \\ v \end{bmatrix} \qquad \text{where} \qquad A_k = \begin{bmatrix} 0 & 1 \\ -1 & 2k \end{bmatrix} = \begin{bmatrix} 1 & 0 \\ 2k & 1 \end{bmatrix} \begin{bmatrix} 0 & 1 \\ -1 & 0 \end{bmatrix}$$

So the squares $Q3$ and $Q4$ are mapped onto the union of $Q4$ and $Q1$. The linear map is hyperbolic there since $\det(A_k) = 1$ and $\mathrm{tr}(A_k) = 2k$ and we have the restriction $|k| \geq 2$. The eigenvalues of A_k are λ_k and λ_k^{-1}, where $|\lambda_k| = |k| + \sqrt{k^2 - 1} > 1$ and $\mathrm{sign}(\lambda_k) = \mathrm{sign}(k)$.

For each k, the map is clearly continuous, piecewise linear and preserves Lebesgue measure. From these considerations, one easily computes that the positive Lyapunov exponent along an orbit is equal to $s \log |\lambda_k|$ where s is the frequency of visits to $Q3 \cup Q4$. Once we establish the ergodicity of T, we get immediately that $s = \frac{1}{2}$ Lebesgue-almost-everywhere.

Although the maps T_k and T_{-k} are not topologically conjugate (as will be explained in Section 3.2), they are related in the following way. Let $D(u, v) = \left(\frac{1}{2} - u, v\right)$ and $E(u, v) = \left(u, \frac{1}{2} - v\right)$ be the reflections across the vertical line $u = 1/4$ and the horizontal line $v = 1/4$, respectively. We have that $D \circ E = E \circ D = C$. The relation between the maps T_k and T_{-k} is given by the following

$$D \circ T_k \circ D = E \circ T_k \circ E = C \circ T_{-k}. \tag{3}$$

Hence although the maps T_k and T_{-k} are not topologically conjugate, their factors by the symmetry C are. This fact will explain the symmetric connection between the Markov partitions for the maps T_k and T_{-k}.

3 Dynamical Properties

In this section we explore some of the dynamical properties of the maps T_k, $|k| \geq 2$, by constructing finite Markov partitions and analyzing the associated symbolic dynamics. As a by-product, we establish that the maps in this family are pseudo-Anosov.

3.1 Invariant foliations

We use the stable and unstable eigenvectors of the matrix A_k to define two invariant piecewise linear foliations $\mathcal{F}^+$ and $\mathcal{F}^-$ for $T = T_k$. Note that in view of the S-reversibility of the map T, and hence also of the linear map A_k, the stable and unstable eigenvectors are exchanged by the reflection S.

We define the foliation $\mathcal{F}^-$ outside of the square $Q2$ to be comprised of segments parallel to the unstable eigenvector of A_k, extended until they intersect the boundary of $Q2$. Inside of the square $Q2$, we define $\mathcal{F}^-$ to be the segments perpendicular to the unstable eigenvector of A_k. Clearly $\mathcal{F}^-$ is invariant on the finite orbits which do not enter $Q2$. The orbits that enter $Q1$ are rotated clockwise by $\pi/2$ and enter $Q2$. They then immediately leave $Q2$ via the same rotation by $\pi/2$, which gives us the invariance of the foliation.

Similarly, we define the stable foliation $\mathcal{F}^+$ by segments, respectively, parallel outside $Q2$ and perpendicular inside $Q2$ to the stable eigenvector of A_k. The stable foliation $\mathcal{F}^+$ can also be obtained from the unstable foliation $\mathcal{F}^-$ by the reflection map S, as should be the case in view of the S-reversibility of the map T. These foliations will allow us to establish that the maps are pseudo-Anosov, as was shown by MacKay, [M], for the case $k = 2$.

We postpone the discussion of the transverse measures required in the definition of pseudo-Anosov maps until we have constructed the Markov partitions.

3.2 Nature of the singularities

The four corners of $Q2$ are singularity points for T, for each value of k. The points $(0, 0)$ and $(-1/2, -1/2)$ are fixed points while $(-1/2, 0)$ and $(0, -1/2)$ make an orbit of period two.

We recall the definition of an n-prong singularity. An isolated singularity p of T is called an *n-prong singularity*, $n = 1, 3, 4, \ldots$, if the local stable and unstable leaves at p are homeomorphic to the curves $Re(z^{n/2}) = const$ and $Im(z^{n/2}) = const$ respectively near $z = 0$ in $\mathbb{C}$. Note that $n = 2$ is not included.

From our definition of the stable and unstable leaves, it follows that the four points mentioned above are singularity points for T. For $k \geq 2$, the two fixed points are 1-prong singularities and the two points of period two are 3-prong singularities. For $k \leq -2$, the nature of the singularities reverses: the two fixed points are 3-prong singularities and the two points of period two are 1-prong singularities. Since the type of singularity is a topological invariant we can see that the maps for k and $-k$ cannot be topologically conjugate.

There are other fixed points for T which are not singular. In fact, the number of fixed points for T increases with $|k|$. By symmetry, fixed points lie on the line $v = u$ and so are easy to find. There are $|k| + 2$ fixed points for $k \leq -2$, and k fixed points for $k \geq 2$. This again implies that the maps for opposite values of k are not topologically conjugate.

3.3 The Markov partition

In [M], a Markov partition with 6 elements was constructed for the map H conjugate to T_2. This was further refined in [G] where it was shown that in fact H admits a 4 element partition. Our Markov partition for T_k also has 4 elements, but it is not generating and is not a generalization of the partitions used in [M, G]. Its advantage lies in its symmetry and universal applicability for all values of k.

The boundaries of our partition elements consist entirely of pieces of the unstable manifolds of the 1-prong singularities and stable manifolds of the 3-prong singularities, which are either fixed points or points of period 2 (depending on the sign of k). This is the basis for the Markov property, just as in the case of Markov partitions for hyperbolic 2-dimensional toral automorphisms, [KH].

We will denote the elements of the partition $\mathcal{P} = \mathcal{P}_k$ by P_1, P_2, P_3, P_4, where the numbering is chosen in such a way that P_2 and P_3 cover mostly (but not exactly) $Q2$ and $Q3$ respectively.

To define P_3 we extend the stable leaves of the two 3-prong singularities, which lie outside $Q2$, until their first intersection with the unstable leaves of the 1-prong singularities. The set P_3 is the parallelogram bounded by the four segments and lying mainly in $Q3$.

We have the symmetry $C(P_3) = P_3$. It is a simple geometric fact that independent of the value of k the area of P_3 is the same as the area of $Q3$, i.e., it is equal to $1/4$. This follows from the fact that the stable and unstable directions are symmetric under the reflection S.

We now define $P_2 = T^{-1}(P_3)$ and $P_4 = T(P_3)$. The set P_1 is the complement of the union $P_2 \cup P_3 \cup P_4$ (more exactly the closure of the complement). Since T is area-preserving, by construction all the elements of our partition have the same area (equal to $1/4$). For clarity, we include figures of the Markov partition and its image for $k = -2$ in Figure 1.

Notice that each of the four pieces of the partition $\mathcal{P}$ is centered at one of the fixed points of C and enjoys the same symmetry $C(P_i) = P_i$.

To see that $\mathcal{P}$ is in fact a Markov partition for T, first consider the following description of its boundary.

(a) The unstable boundaries of the four elements lie entirely on segments of the unstable leaves of the two 1-prong singularities. These segments can be described as follows. The unstable leaf is extended until it crosses the boundary of $Q2$. It stops at its first intersection *inside* $Q2$ with the stable manifold of one of the 3-prong singularities. Incidentally these segments constitute the complete unstable boundaries of the "longest" element P_1. At the 1-prong singularities the boundary of P_1 has a "fold" which we prefer to consider as cut open.

(b) The stable boundaries of the four elements lie entirely on segments of the stable leaves of the 3-prong singularities. These segments are obtained by extending the stable leaves until their first intersection *outside of* $Q2$ with the unstable manifold of the 1-prong singularities. In this case all of the stable boundaries are contained in the stable boundaries of P_2 and P_3.

Remark 3.1. *Although Figure 1 shows $\mathcal{P}$ for $k = -2$, the structure of $\mathcal{P}$ remains essentially the same for each value of k. The modifications for other values of k are as follows.*

As $|k|$ increases, so does $|\lambda_k|$ and the unstable leaves of A_k outside of $Q2$ become close to vertical and the stable leaves become close to horizontal. Hence for large $|k|$, P_3 almost

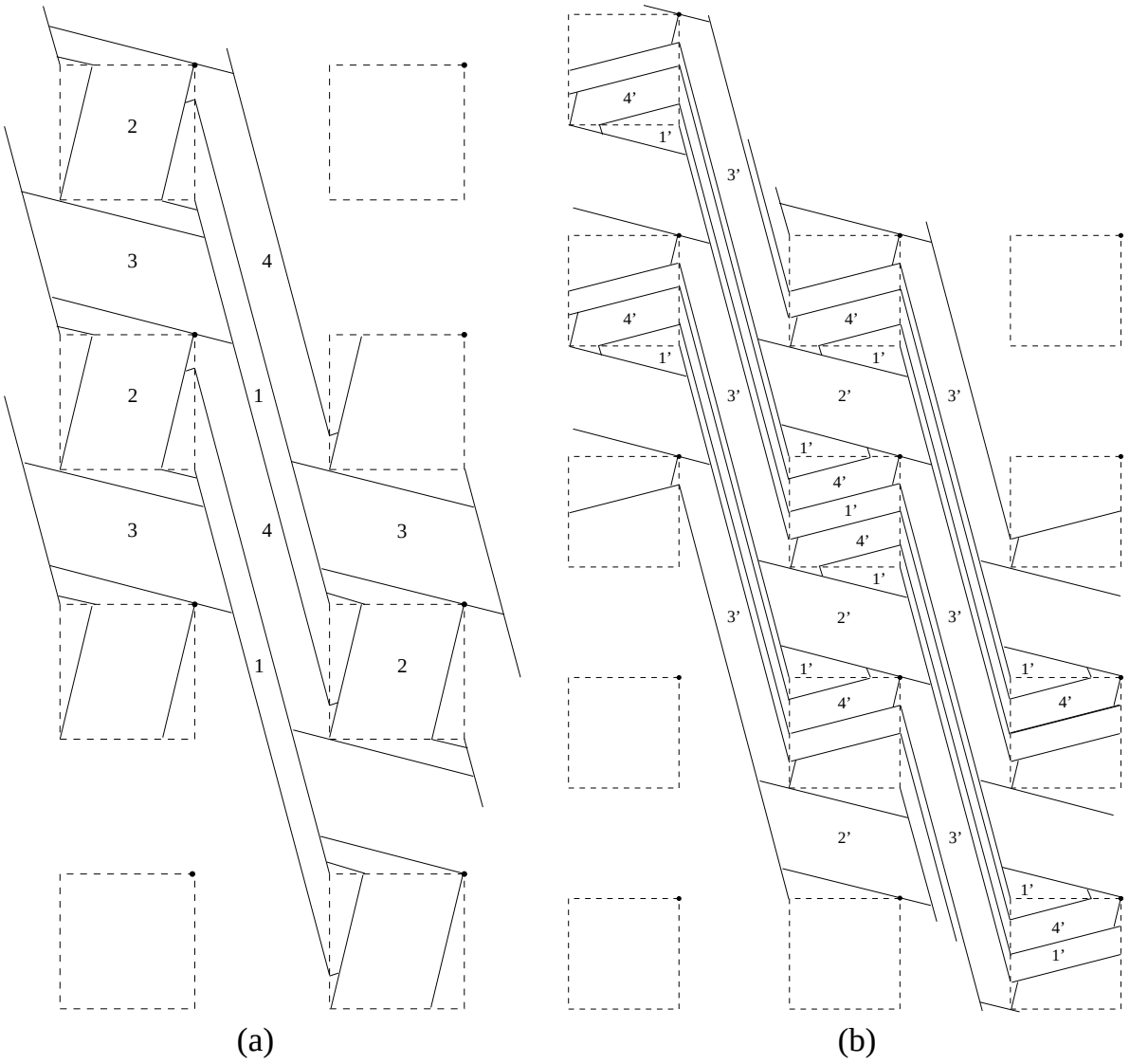

Figure 1: (a) A 4 element Markov partition for $k = -2$ and (b) its image.

(a) The partition elements follow the numbering described above so that $T(3) = 4$, $T(2) = 3$ and element 1 is the complement of the first three. The dotted square represents the boundary of $Q2$ where $\mathcal{F}^+$ and $\mathcal{F}^-$ change direction by $\pi/2$. Its corners are the 4 singularity points and the emphasized dot represents the origin.
(b) The image of each element j is labeled j'.

coincides with the square $Q3$. The slopes of the stable and unstable leaves are positive for $k \geq 2$ and negative for $k \leq -2$.

P_4 and P_1 become longer as $|k|$ increases so that P_4 runs past $|k|$ copies of the square $Q2$ while P_1 runs past $|k|+1$ copies of $Q2$. The images of $P_1 \cap Q4$ and $P_4 \cap Q4$ are expanded by a factor of $|\lambda_k|$ so that the number of intersections with $Q2$ increases linearly with $|k|$.

We recall the two defining features of a Markov partition in two dimensions: (1) Each element of $\mathcal{P}$ has a local product structure: the local stable and unstable manifolds of any two points in a given element have a unique point of intersection in that element; (2) The boundary of the partition is a union of stable and unstable leaves, denoted $\partial\mathcal{P}^+$ and $\partial\mathcal{P}^-$ respectively, satisfying: $T(\partial\mathcal{P}^+) \subset \partial\mathcal{P}^+$ and $T^{-1}(\partial\mathcal{P}^-) \subset \partial\mathcal{P}^-$.

For our partition, the first condition follows immediately from the fact that the boundary of each element of $\mathcal{P}$ has four "sides," an alternating arrangement of two stable and two unstable curves. The second condition is also fairly straight forward. For $k \geq 2$, we use the unstable manifolds of the fixed points for $\partial\mathcal{P}^-$ so it is automatic that $T^{-1}(\partial\mathcal{P}^-) \subset \partial\mathcal{P}^-$. For $k \leq -2$, we use the unstable manifolds of the points of period two so that one unstable segment is mapped into the other by T^{-1}. But since they begin with comparable lengths and each shrinks by a factor of λ^{-1}, they do map strictly inside one another. Similar considerations show that the stable manifolds of the 3-prong singularities map inside one another under the action of T.

A second way to check that $\mathcal{P}$ is Markov is to use the fact that $T(P_3) = P_4$ and $T(P_2) = P_3$. So the $\mathcal{F}^+$ (stable) boundaries of P_2 and P_3 automatically satisfy requirement (2) for a Markov partition. But the $\mathcal{F}^+$ boundaries of P_1 and P_4 are contained in those of P_2 and P_3 by (b) above so there is nothing left to check for $\partial\mathcal{P}^+$. For $\partial\mathcal{P}^-$, the fact that $T^{-1}(P_3) = P_2$ and $T^{-1}(P_4) = P_3$ implies that the $\mathcal{F}^-$ (unstable) boundaries of P_3 and P_4 satisfy requirement (2). The only part of $\partial\mathcal{P}^-$ left to check are two short unstable segments coming out of the 1-prong singularities before they intersect one of the stable sides of P_3. Since these two segments have the same length (by symmetry) and are each contracted by a factor of λ^{-1} in one application of T^{-1}, they map strictly inside one another if $k \leq -2$ and strictly inside themselves if $k \geq 2$.

The partition $\mathcal{P}$ also enjoys the following symmetry. Recall that the nature of the 1 and 3-prong singularities is reversed when we switch from positive to negative k. Thus if we follow the change in 1 and 3-prong singularities and switch the roles of stable and unstable manifolds in our partition for T_k, we get the corresponding partition for T_{-k}.

To be precise, once the Markov partition $\mathcal{P}_k = \{P_1, P_2, P_3, P_4\}$ for a given value of k is constructed, we obtain the Markov partition of the map for the opposite value $-k$ by applying the reflection D (or E), i.e, $\mathcal{P}_{-k} = \{D(P_1), D(P_2), D(P_3), D(P_4)\}$. The Markov property of one follows from the Markov property of the other using the symmetries (1) and (3). Indeed D takes stable leaves of T_{-k} into stable leaves of T_k, and unstable into unstable.

3.3.1 Connectivity matrix

Once the existence of a finite Markov partition has been established, we know that T is nearly conjugate to a topological Markov chain whose dynamics are described by a connectivity matrix. Since the partition is not generating, we count the number of connected intersections with the image of each piece separately.

From Figure 1, we can easily read off the connectivity matrix and notice the pattern for the family of maps T_k since the structure of the partition remains essentially unchanged (see Remark 3.1). Indeed, the connectivity matrix is given by

$$M_k = \begin{bmatrix} |k| & |k|+1 & 0 & 0 \\ 0 & 0 & 1 & 0 \\ 0 & 0 & 0 & 1 \\ |k|-1 & |k| & 0 & 0 \end{bmatrix}$$

where the $(i,j)^{\text{th}}$ entry of M_k, denoted $M_k(i,j)$, is the number of connected components of $T(P_i) \cap P_j$. The simple structure of the matrix follows from the fact that $T(P_2) = P_3$ and $T(P_3) = P_4$.

The characteristic polynomial is $t^4 - |k|t^3 - |k|t + 1$ and the top eigenvalue is given by

$$\alpha_k = \frac{|k| + \sqrt{k^2+8} + \sqrt{-8 + 2k^2 + 2|k|\sqrt{k^2+8}}}{4}. \tag{4}$$

It follows immediately that the topological entropy of T_k is given by $h_{\text{top}}(T_k) = \log \alpha_k$ for each k.

In addition, Lebesgue measure is the SRB measure of the system. In Section 4.2 we will establish that its metric entropy is equal to $h_m(T_k) = \frac{1}{2} \log |\lambda_k|$ so that Pesin's formula holds.

3.4 Maps T_k are pseudo-Anosov

3.4.1 Definition of pseudo-Anosov

Recall that a homeomorphism f of a compact surface is called *pseudo-Anosov* if it possesses a uniformly transverse pair of foliations $\mathcal{F}^+$ and $\mathcal{F}^-$ with transverse measures μ^+ and μ^- which are expanded by a constant factor $\alpha > 1$ at each iteration of f and f^{-1}, respectively. In addition, f has a finite nonempty set of n-prong singularities.

Pseudo-Anosov maps were introduced by Thurston [T] and have well-established properties. In particular, it is known that such maps possess finite Markov partitions, are topologically mixing with positive topological entropy, $h_{top}(f) = \log \alpha$, and possess a measure of maximal entropy μ which is the product of the two transverse measures $\mu^{\pm}$ (for further properties, see also [Bo, CB]). Pseudo-Anosov homeomorphisms with quadratic α and even-pronged singularities are known to be semi-conjugate to a hyperbolic toral automorphism [FR]; note that for our T_k, α is quartic (4) and our singularities are odd-pronged.

3.4.2 Description of transverse measures

The invariant foliations $\mathcal{F}^+$ and $\mathcal{F}^-$ required by the definition of pseudo-Anosov are the stable and unstable foliations, respectively, defined in Section 3.1. We have already seen in Section 3.2 that the 4 singularities of T_k are of the type required for a pseudo-Anosov map. It remains to provide the transverse measures μ^+ and μ^-. Since we have already constructed the Markov partition for our maps we can use the standard procedure as in [M] adapted to a nongenerating partition.

We define μ^+ on $\mathcal{F}^+$ as follows. Since $M = M_k$ is a nonnegative, mixing matrix for each $|k| \geq 2$, we know from Perron-Frobenius theory that there exists a unique positive right eigenvector $\vec{p}$ corresponding to the largest eigenvalue $\alpha = \alpha_k$, given by (4). There also exists a unique positive left eigenvector $\vec{q}$ corresponding to α. We assume both are normalized so that their components sum to one.

On each element of $\mathcal{P}$, we define $\mu^+(P_i) = \vec{p}(i)$, i.e. the set of all (local) leaves in $\mathcal{F}^+$ crossing P_i has weight equal to the i^{th} component of the vector $\vec{p}$.

We define the weight of an arbitrary subinterval I of leaves of $\mathcal{F}^+$ crossing a given region in terms of cylinder sets.

We call R a *u-subset* (resp. *s-subset*) if R lies entirely in one of the elements P_i of $\mathcal{P}$ and has the property that any unstable (stable) leaf in R extends fully across P_i.

Let $R = [i_0, \ldots, i_r]$ be a cylinder set with respect to $\bigvee_{j=0}^r T^{-j}\mathcal{P}$, i.e. $R = \bigcap_{j=0}^r T^{-j} P_{i_j}$. The cylinder R is an s-subset in P_{i_0} corresponding to a subset of (local) leaves $\mathcal{F}^+$. The number $c(R)$ of connected components of R can be expressed in terms of the connectivity matrix, namely

$$c(R) = M(i_0, i_1) \cdots M(i_{r-1}, i_r).$$

We put $\mu^+(R) = \alpha^{-r} c(R) \vec{p}(i_r)$. Further we give the weight of $\alpha^{-r}\vec{p}(i_r)$ to the set of (local) leaves comprising each of the $c(R)$ components of R. It follows immediately from this description that μ^+ is expanded uniformly by a factor of α at each iterate of T.

It is straightforward to check that μ^+ is additive on cylinder sets. Since $[i_0, \ldots, i_{r-1}] = \bigcup_{i=1}^4 [i_0, \ldots, i_{r-1}, i]$, we have

$$\begin{aligned} \sum_{i=1}^4 \mu^+([i_0, \ldots, i_{r-1}, i]) &= \sum_{i=1}^4 \alpha^{-r} M(i_0, i_1) \cdots M(i_{r-1}, i) \vec{p}(i) \\ &= \alpha^{-r} M(i_0, i_1) \cdots M(i_{r-2}, i_{r-1}) \alpha \vec{p}(i_{r-1}) \;=\; \mu^+([i_0, \ldots, i_{r-1}]) \end{aligned}$$

where in the last line, we have used the fact that $\vec{p}$ is a right eigenvector for M.

Similarly, one defines μ^- on $\mathcal{F}^-$ using as weights the entries of the left eigenvector $\vec{q}$. Since the connectivity matrix for T^{-1} is the transpose of M, α remains the top eigenvalue and the measure μ^- enjoys the same uniform expansion as μ^+ by a factor of α at each iterate of T^{-1}. Alternatively, since $\mathcal{F}^-$ is simply $\mathcal{F}^+$ reflected across the line $u = v$, one can define μ^- from μ^+ by applying the reflection S.

Remark 3.2. *The measure μ^+ can be realized as the limit of various dynamical quantities. One is the following: Fix r and let $R \in \bigvee_{j=0}^r T^{-j}\mathcal{P}$. For $n \geq 0$, let $\zeta_n(k)$, $k = 1, 2, \ldots$, be the finite sequence of labels of the elements of $\mathcal{P}$ completely crossed in the unstable direction by $T^n(R)$, repeated according to the number of crossings. Then $\mu^+(R) = \lim_{n\to\infty} \alpha^{-n} \sum_k \vec{p}(\zeta_n(k))$. The proof of this is standard (c.f. [KH, Chapter 4]). We give two more equivalent characterizations in the next section.*

3.4.3 Connection to a physical measure

The transverse measures μ^+ and μ^- represent the asymptotic distributions of long segments of leaves in $\mathcal{F}^+$ and $\mathcal{F}^-$ respectively, which goes back to Margulis [KH]. Let us make this connection explicit.

It is a standard consequence of the Perron-Frobenius theorem (see, for example, [KH]) that

$$\lim_{n\to\infty} \alpha^{-n} M^n(i,j) = \vec{p}(i)\vec{q}(j) / \Big(\sum_i \vec{p}(i)\vec{q}(i) \Big). \tag{5}$$

We define a type of counting measure ν^+ as follows. For a point z let $i(z)$ be its label, i.e., $z \in P_{i(z)}$ and let $\omega_0(z)$ be an element of $\mathcal{F}^+|_{P_{i(z)}}$, i.e. a full stable leaf in $P_{i(z)}$. We consider the long segments of leaves in $\mathcal{F}^+$, $\omega_n(z) = T^{-n}\omega_0(T^n z)$ and define its asymptotic distribution as follows. Let

$$N_n(P_j) = \#\text{ of times } \omega_n(z) \text{ crosses } P_j$$

and notice that $N_n(P_j) = M^n(j, i(T^n z))$ since the connectivity matrix for T^{-1} is the transpose of M. Let $N_n = \sum_{j=1}^4 N_n(P_j)$ denote the total number of crossings by $\omega_n(z)$. Then the asymptotic proportion of the number of crossings of P_j by the complete stable leaf through z is given by

$$\nu^+(P_j) = \lim_{n\to\infty} \frac{M^n(j, i(T^n z))}{\sum_{r=1}^4 M^n(r, i(T^n z))} = \lim_{n\to\infty} \frac{\alpha^{-n} M^n(j,i)}{\alpha^{-n} \sum_{r=1}^4 M^n(r,i)} = \frac{\vec{p}(j)\vec{q}(i)}{\sum_{r=1}^4 \vec{p}(r)\vec{q}(i)} = \vec{p}(j)$$

where we have split the sequence into subsequences with constant value of $i(T^n z) = i$, and used (5) to evaluate the limit.

Notice that the limit is independent of the choice of z and that it agrees with μ^+ on partition elements.

We now establish that ν^+ and μ^+ are equal on connected s-subsets and are therefore equal as measures. Let S be an s-subset which is a connected component of an $(r+1)$-cylinder, $R = [i_0, \ldots, i_r]$.

We must count the number of times $\omega_n(z)$ crosses S. Notice that the number of crossings of R by $\omega_n(z)$ is equal to the number of crossings of P_{i_r} by $\omega_{n-r}(z)$ multiplied by $c(R) = M(i_0, i_1) \cdots M(i_{r-1}, i_r)$, the number of connected components in R. Thus for a single connected component, $N_n(S) = N_{n-r}(P_{i_r})$.

$$\begin{aligned} \nu^+(S) &= \lim_{n\to\infty} \frac{N_{n-r}(P_{i_r})}{N_n} = \lim_{n\to\infty} \alpha^{-r} \frac{\alpha^{r-n} M^{n-r}(i_r, i(T^{n-r}z)}{\alpha^{-n} \sum_{j=1}^4 M^n(j, i(T^{n-r}z)} \\ &= \alpha^{-r} \vec{p}(i_r) = \mu^+(S) \end{aligned}$$

where again we have used (5).

Remark 3.3. *The measure ν^+ is obtained by growing the local stable leaf of a single point. The same measure is also defined by applying T^{-n} to a single stable leaf and measuring its asymptotic distribution. In the notation above, fix $\omega \in \mathcal{F}^+|_{P_i}$ and let $N_i^n(P_j)$ denote the number of times $T^{-n}\omega$ crosses P_j. The calculations of $\nu^+(P_j)$ and $\nu^+(S)$ follow as above.*

3.4.4 Quantification of multifractality

We can quantify the fractality of the measure μ_+ in the same way as was done in [M]. Let us fix a smooth transversal J to the stable foliation $\mathcal{F}^+$, say a piece of unstable leaf. For

a point $x \in J$, let $J^n(x)$ be the interval corresponding to the connected component of the cylinder set $[i_0, i_i, \ldots, i_n]$ containing x. It follows from the definition of μ^+ that

$$\lim_{n\to+\infty} \frac{1}{n} \log \mu^+(J^n(x)) = -\log \alpha_k.$$

On the other hand for the Lebesgue measure of the interval $|J^n(x)|$ and the positive Lyapunov exponent $\chi(x)$, we have

$$\lim_{n\to+\infty} \frac{1}{n} \log |J^n(x)| = -\chi(x).$$

It follows that the pointwise dimension $\delta(x)$ of μ^+ is given by,

$$\delta(x) = \lim_{n\to+\infty} \frac{\log \mu^+(J^n(x))}{\log |J^n(x)|} = \frac{\log \alpha_k}{\chi(x)}.$$

For Lebesgue-almost-every point $x \in J$, the Lyapunov exponent $\chi(x) = \frac{\log|\lambda_k|}{2}$ and hence the pointwise dimension is $\delta(x) = \frac{2\log\alpha_k}{\log|\lambda_k|}$. Using (4), one can easily calculate that this pointwise dimension is larger than 1 and increases to 2 as the shearing coefficient k tends to infinity.

4 Simplified Analysis via Reduction to Two States

In this section we describe explicitly the connection between T and a related family of toral automorphisms. By rectifying the elements of our Markov partition $\mathcal{P}$, we show that T can be viewed as an extension of a map $\widetilde{T}$ which is metrically equivalent to and generates the same Markov process as the toral automorphism defined by its transition matrix. This in turn allows us to compute directly the Hausdorff dimensions of the level sets of the positive Lyapunov exponent.

4.1 Rectification of the Markov partition

The element P_3 is a parallelogram, the other pieces are not. This is consistent with the fact that the stable and unstable leaves are piecewise linear, but not linear. However both $P_2 = T^{-1}(P_3)$ and $P_4 = T(P_3)$ can be considered as being geometric parallelograms. The map T itself, being piecewise linear, provides the geometric coordinates in which the "ends" of P_2 and P_4 can be straightened. There is another way to achieve the same goal: the two ends in $P_2 \setminus Q_2$ can be sheared into position so that the stable and unstable leaves in P_2 become straight and the piece turns into a parallelogram. By a shear we mean a linear map with a double eigenvalue 1. Note that we have not changed the element in the "middle", i.e., $P_2 \cap Q_2$ stays the same. The resulting parallelogram is congruent to P_3 under the clockwise rotation by $\pi/2$ about its center. We will rotate the rectified piece by this angle, and denote the obtained parallelogram by R_2. In the same way the element P_4 can be turned into the parallelogram R_4 by shearing. We do not rotate R_4.

We claim that P_1 also can be turned into a parallelogram by shearing. Since this is obviously the most complex of the pieces to rectify, we will describe this procedure precisely and give an argument which is independent of k. For clarity, Figure 2 illustrates the process

in the case $k = -2$. Indeed, it suffices to give the details for one end of P_1 since the other end can be rectified following the same steps by symmetry. We will refer to the named points of Figure 2 throughout the following construction.

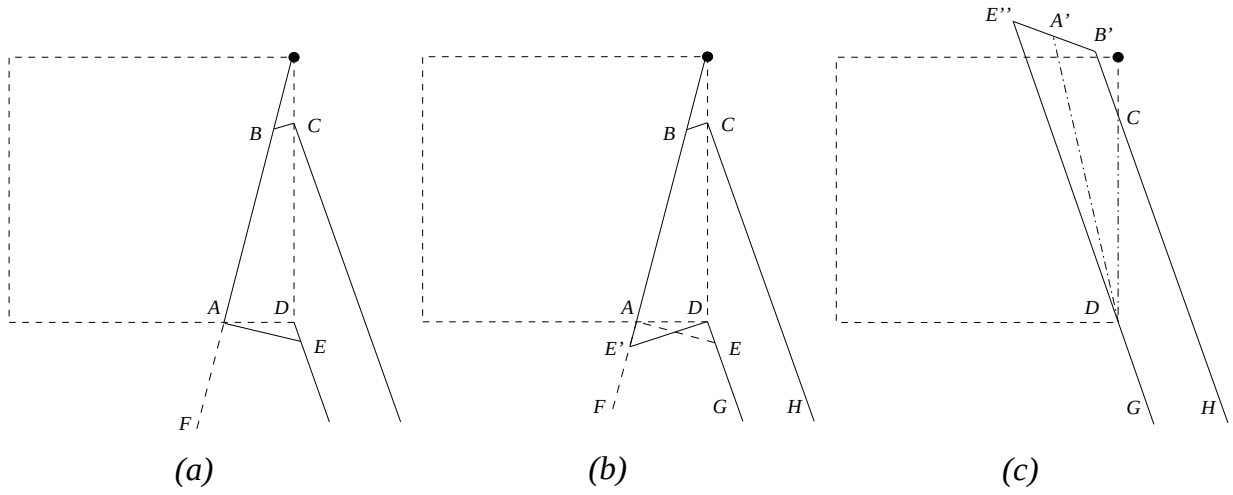

Figure 2: One end of P_1 and its image after each shear.

(a) One end of P_1 showing the cut along segment DE. The stable boundary is given by BAE; BC and the two segments extending downwards from C and D belong to the unstable boundary. As in Figure 1, the dotted square represents the boundary of $Q2$.
(b) $\triangle ADE$ after the first shear has become $\triangle ADE'$. The stable boundary has been straightened.
(c) Quadrilateral $DCBE'$ has been sheared into $DCB'E''$, straightening both unstable boundaries simultaneously. Edge $B'E''$ is now parallel to the stable direction of T outside of $Q2$. The dash-dot line DA' represents the image of the boundary of the domain on which the first shear acted; DC is the boundary of the domain for the second shear.

Step 1. We first cut open P_1 along the singular unstable leaf of the 1-prong singularity from point D to point E (Fig. 2(a)). Our goal is to shear $\triangle ADE$ so that segment AD is kept invariant and the image E' of E lies on the segment BF which is an extension of BA. Thus we are straightening the stable boundary BAE. Notice that by definition of $\mathcal{F}^+$, BF is perpendicular to AE.

The stable eigenvector of A_k is $\vec{v}_s = \begin{bmatrix} 1 \\ \lambda^{-1} \end{bmatrix}$ and by definition of $\mathcal{F}^+$, this gives the direction of AE. Recall that λ satisfies

$$\lambda^2 - 2k\lambda + 1 = 0 \qquad \text{so} \qquad \lambda + \lambda^{-1} = 2k. \tag{6}$$

For the first shear, *we consider A as the origin of our coordinate system* and let

$$L_1 = \begin{bmatrix} 1 & -2k \\ 0 & 1 \end{bmatrix}.$$

Since by (6),

$$L_1\vec{v}_s = -\lambda^{-1}\begin{bmatrix} -\lambda + 2k \\ -1 \end{bmatrix} = -\lambda^{-1}\begin{bmatrix} \lambda^{-1} \\ -1 \end{bmatrix},$$

which is perpendicular to $\vec{v}_s$, we know that AE' lies on AF as required.

Due to the symmetries of $\mathcal{P}$, we also have the following important lemma.

Lemma 4.1. *DE' is parallel to BC.*

Proof. Recall that BC is perpendicular to DE by definition of $\mathcal{F}^-$. Since AD is invariant under L_1 and DE is parallel to the unstable eigenvector $\vec{v}_u = \begin{bmatrix} 1 \\ \lambda \end{bmatrix}$, the direction of DE' must be given by $L_1\vec{v}_u$. This is

$$L_1\vec{v}_u = \begin{bmatrix} 1-2k\lambda \\ \lambda \end{bmatrix} = \lambda \begin{bmatrix} -\lambda \\ 1 \end{bmatrix}$$

again using (6). Thus DE' is perpendicular to DE and so parallel to BC. □

The importance of this lemma lies in the fact that since DE' is parallel to BC, a single shear will align both segments with HC and GD, which otherwise might not have been possible (see Figure 2(b)).

Step 2. Our goal in this step is to use a single shear which will simultaneously straighten HCB and GDE' while aligning BE' with the stable direction given by $\vec{v}_s$. (See Figure 2(b) and (c).)

For the second shear, *we consider D to be the origin of our coordinate system* and let

$$L_2 = \begin{bmatrix} 1 & 0 \\ 2k & 1 \end{bmatrix}.$$

Since DE' is parallel to $\begin{bmatrix} \lambda \\ -1 \end{bmatrix}$, its image under L_2, DE'', must be parallel to

$$L_2 \begin{bmatrix} \lambda \\ -1 \end{bmatrix} = \begin{bmatrix} \lambda \\ 2k\lambda - 1 \end{bmatrix} = \lambda \begin{bmatrix} 1 \\ \lambda \end{bmatrix}$$

which is parallel to $\vec{v}_u$. Thus GDE'' is a straight line.

Since BC is parallel to DE' and DC is invariant under L_2 in our chosen coordinates, the image $B'C$ of BC is also parallel to $\vec{v}_u$. Thus HCB' is also a straight line.

It remains to show that $B'E''$ is parallel to $\vec{v}_s$. Recall from Step 1 that BE' is parallel to $\begin{bmatrix} \lambda^{-1} \\ -1 \end{bmatrix}$. Now

$$L_2 \begin{bmatrix} \lambda^{-1} \\ -1 \end{bmatrix} = \begin{bmatrix} \lambda^{-1} \\ 2k\lambda^{-1} - 1 \end{bmatrix} = \lambda^{-1}\vec{v}_s,$$

again using (6). Thus $B'E''$ is parallel to $\vec{v}_s$ as required.

The net result after shearing both ends of P_1 is a parallelogram, which we denote by R_1, with two sides parallel to $\vec{v}_u$ and two sides parallel to $\vec{v}_s$.

Thus we get four parallelograms R_1, R_2, R_4 and $R_3 = P_3$, which we place apart, i.e., with no mutual intersections, in one plane so that the stable boundaries (and unstable boundaries) of the four pieces are parallel. Choosing the scalar product appropriately we

can make the stable boundaries and unstable boundaries perpendicular to each other. For example the stable boundaries are horizontal and the unstable boundaries are vertical. The parallelograms become rectangles.

The map T in this representation is still piecewise linear. Up to translations and/or rotation by $\pi/2$ these are the same linear maps as before. Moreover, in our new coordinates the linear map A_k is diagonal with λ and λ^{-1} on the diagonal. To see this, it is useful to invoke the following lemma, which we state without proof.

Lemma 4.2. *An invertible area preserving map from a rectangle in $\mathbb{R}^2$, with horizontal and vertical sides, into $\mathbb{R}^2$ which takes horizontal segments into horizontal segments and vertical segments into vertical segments, must be linear.*

By the lemma the map T is linear on each separate rectangle in $R_i \cap T^{-1}R_j$. It is also linear on each of the pieces which were sheared, or left alone, during the process of rectification described above. Since these two ways of partitioning the rectangles have no common pieces (see Figure 2(c)), we are able to make the following conclusions:

1. The map T translates R_2 onto R_3 because to obtain R_2 we have rotated P_2 clockwise by $\pi/2$. Hence the derivative of T on R_2 is equal to the identity I.
2. On R_3 the derivative of T is equal to A.
3. On $R_4 \cap T^{-1}R_1$ the derivative is A while on $R_4 \cap T^{-1}R_2$ it is equal to minus identity $-I$ (the rotation by π), since R_2 is the rectified P_2 rotated clockwise by an additional angle of $\pi/2$.
4. On $R_1 \cap T^{-1}R_2$ the derivative of T is $-I$ while on $R_1 \cap T^{-1}R_1$ it is A.

These relations are summarized in Figure 3.

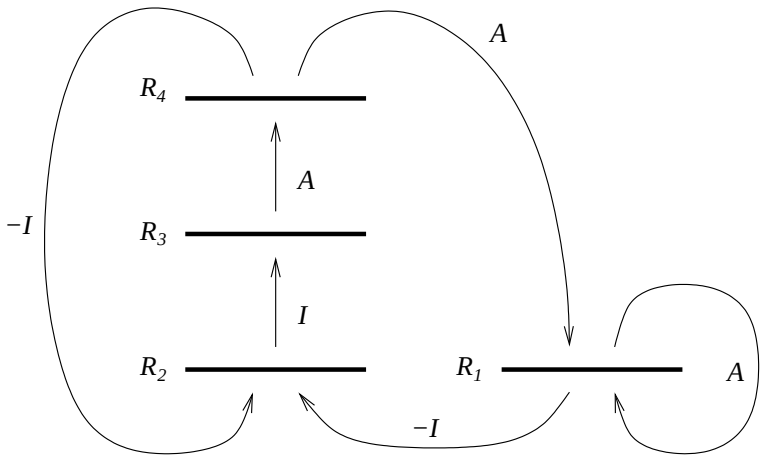

Figure 3: Schematic of the map T on 4 rectangles.

4.2 A return map for T

According to Figure 3, we consider R_1, R_2, R_3 and R_4 as forming a tower of height 2 over the base $R_1 \cup R_2$. We define the return map $\widetilde{T} : R_1 \cup R_2 \circlearrowleft$ by $\widetilde{T}|_{R_1} = T$ and $\widetilde{T}|_{R_2} = T^3$. It is again piecewise linear. Its derivative can be obtained directly from of the determination of the derivative of T above. In particular for $p \in R_1 \cap \widetilde{T}^{-1}R_1$, the derivative $D_p\widetilde{T} = A$. On $R_2 \cap \widetilde{T}^{-1}R_1$ it is equal to A^2 while on $R_1 \cap \widetilde{T}^{-1}R_2$ it is equal to $-I$. Finally on $R_2 \cap \widetilde{T}^{-1}R_2$, the derivative is equal to $-A$.

The return map $\widetilde{T}$ is a Markov map on the two rectangles $R_1 \cup R_2$. We can find the connectivity matrix $\widetilde{M} = \widetilde{M}_{|k|}$ directly from the matrix M_k given in Section 3.3.1 for the 4 element partition:

$$\widetilde{M}_{|k|} = \begin{bmatrix} |k| & |k|+1 \\ |k|-1 & |k| \end{bmatrix},$$

where the $(i,j)^{\text{th}}$ entry of $\widetilde{M}$, is the number of connected components of $\widetilde{T}(R_i) \cap R_j$. The larger eigenvalue of this matrix is the same as that of A_k (up to sign).

Let us change variables in R_1 one more time. Namely we identify R_1 with $\widehat{R}_1 = A^{-1}R_1$. We will consider this identification to be just a change of coordinates (the coordinates in R_2 stay the same), and we will denote the resulting rectangle again by R_1. In these new coordinates the derivative of the mapping $\widetilde{T}$ is equal to:

$$-A \text{ on } R_1 \cap \widetilde{T}^{-1}R_2 \text{ and } R_2 \cap \widetilde{T}^{-1}R_2; \qquad \text{and} \qquad A \text{ on } R_2 \cap \widetilde{T}^{-1}R_1 \text{ and } R_1 \cap \widetilde{T}^{-1}R_1. \quad (7)$$

We have thus achieved that the derivative of $\widetilde{T}$ is equal to $\pm A$. We see immediately that the metric entropy of $\widetilde{T}$ (with respect to area measure) is equal to $\log|\lambda|$. Since the average return time to $R_1 \cup R_2$ is equal to 2, it follows from the Abramov formula that the metric entropy of T is equal to $\frac{1}{2}\log|\lambda|$.

4.2.1 Connection to a toral automorphism

The matrix $\widetilde{M} = \widetilde{M}_{|k|}$ is an integer matrix with determinant one and eigenvalues equal to $|\lambda|$ and $|\lambda|^{-1}$. Hence it defines a hyperbolic toral automorphism which we denote by $m : \mathbb{T}^2 \to \mathbb{T}^2$. There is an affinity between the mapping $\widetilde{T}$ and the toral automorphism m. Indeed since their metric entropies with respect to the area measure are equal and both are metrically isomorphic to Bernoulli systems, then by Ornstein's Theorem they must be metrically isomorphic. There is actually an even stronger connection.

The mapping $\widetilde{T}$, the partition $\{R_1, R_2\}$, and the normalized area define a stochastic process which we denote by ξ. The process ξ is the double sided stationary Markov chain obtained from the connectivity matrix $\widetilde{M}$ by the Parry recipe. Indeed let us denote by p_1, p_2 the lengths of the unstable (vertical) and by q_1, q_2 the lengths of the stable (horizontal) sides of R_1 and R_2 respectively. Then for any sequence $(i_0, i_1, \ldots, i_n)$ of 1's and 2's the cylinder set

$$R_{i_0} \cap \widetilde{T}^{-1}R_{i_1} \cap \cdots \cap \widetilde{T}^{-n}R_{i_n}$$

is the union of $\widetilde{M}^n(i_0, i_n)$ horizontal rectangles with area equal to $|\lambda|^{-n}q_{i_0}p_{i_n}$, where $\widetilde{M}^n(i_0, i_n)$ is the (i_0, i_n) element of $\widetilde{M}^n$. Further, the shapes of R_1 and R_2 can be read off from $\widetilde{M}$.

Namely, $\vec{p} = (p_1, p_2)$ is the right eigenvector and $\vec{q} = (q_1, q_2)$ is the left eigenvector of $\widetilde{M}$, with eigenvalue $|\lambda|$. To see this, note that since $D\widetilde{T} = \pm A$ by (7), the lengths of the unstable sides are multiplied by $|\lambda|$ under the application of $\widetilde{T}$. This yields the equations

$$|\lambda|p_1 = |k|p_1 + (|k|+1)p_2 \qquad \text{and} \qquad |\lambda|p_2 = (|k|-1)p_1 + |k|p_2. \tag{8}$$

Similarly the lengths of stable sides are multiplied by $|\lambda|^{-1}$ under the application of $\widetilde{T}$ and we get the equations

$$q_1 = |k||\lambda|^{-1}q_1 + (|k|-1)|\lambda|^{-1}q_2 \qquad \text{and} \qquad q_2 = (|k|+1)|\lambda|^{-1}q_1 + |k||\lambda|^{-1}q_2. \tag{9}$$

Direct calculation shows that the eigenvectors are $\vec{p} = \left(\sqrt{|k|+1}, \sqrt{|k|-1}\right)$ and $\vec{q} = \left(\sqrt{|k|-1}, \sqrt{|k|+1}\right)$ (both equalities up to a scalar factor). Thus the rectangles R_1 and R_2 can be made congruent by the rotation by $\frac{\pi}{2}$ (scaling appropriately the stable and unstable sides).

Note that the Markov chain ξ is only a factor of $\widetilde{T}$, since the partition is not generating.

Proposition 4.3. *There is a Markov partition for the toral automorphism m consisting of two rectangles linearly equivalent to R_1 and R_2 such that the resulting Markov chain is equal to ξ.*

Proof. By a theorem of Adler [A, Theorem 8.4], m has a (nongenerating) Markov partition $\mathcal{Q} = (Q_1, Q_2)$ such that Q_1 and Q_2 are parallelograms and the matrix $\widetilde{M}$ itself is the connectivity matrix for this partition. The normalized area is the measure of maximal entropy for m. This measure, the partition $\mathcal{Q}$ and m define a stochastic process equal to the Parry Markov chain obtained from $\widetilde{M}$, and hence equal to ξ.

Equations (8) and (9) apply equally well to the sizes of the stable and unstable sides of Q_1 and Q_2. Hence R_1 and R_2 can be taken onto Q_1 and Q_2 by the same linear map, i.e., they are linearly equivalent. □

By the last Proposition we can consider both the mapping $\widetilde{T}$ and the toral automorphism m as defined on the union of the same two rectangles R_1 and R_2. The stochastic processes defined by the partition and $\widetilde{T}$ and m, respectively, are identical. In particular, for any sequence $(i_0, i_1, \ldots, i_n)$ of 1's and 2's the sets

$$R_{i_0} \cap \widetilde{T}^{-1}R_{i_1} \cap \cdots \cap \widetilde{T}^{-n}R_{i_n} \qquad \text{and} \qquad R_{i_0} \cap m^{-1}R_{i_1} \cap \cdots \cap m^{-n}R_{i_n}$$

are unions of $\widetilde{M}^n(i_0, i_n)$ horizontal strips inside R_{i_0} (each of area $|\lambda|^{-n}q_{i_0}p_{i_n}$). However these sets are **not** equal. They differ in the placement of the horizontal strips. In particular, for both maps, R_1 and R_2 are split into $4|k|$ horizontal strips which form a generating Markov partition. Each horizontal strip is mapped into a vertical strip. The vertical strips are individually isometric for the two maps, but their placements in R_1 and R_2 differ by a permutation and possibly a rotation by π, depending on the sign of k. Figure 4 shows the 8 horizontal strips and their images for $\widetilde{T}$ and m in the case $k = -2$. The figure reveals the symmetry enjoyed by our maps $\widetilde{T}_k$, which is not shared by m.

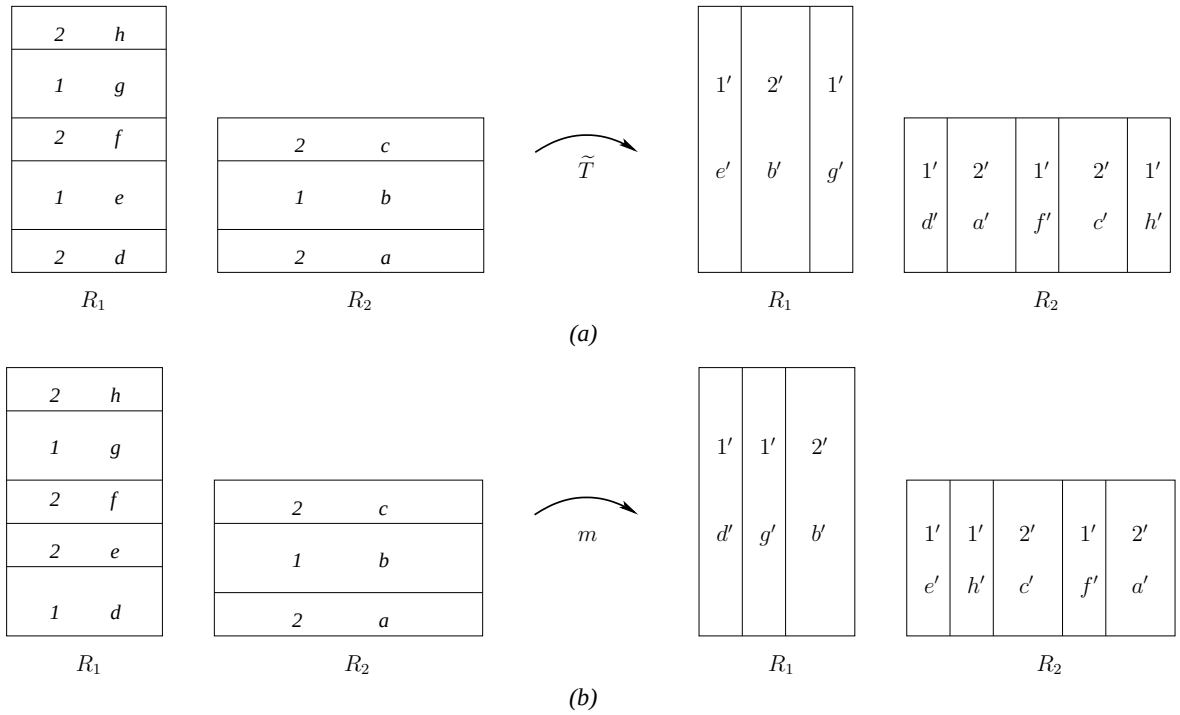

Figure 4: The generating partition and its image for (a) $\widetilde{T}$ and (b) m in the case $k = -2$. The elements of the partition are labeled a-f while the numbers indicate whether each element is mapped into R_1 or R_2. The image of each element is indicated by a prime.

4.3 Dimensional characteristics of the dynamics

MacKay [M] used his Markov partition to explain various features of the map T observed by Cerbelli and Giona, [CG]. In particular he considered the one dimensional map U defined on the "skeleton". The skeleton is obtained by collapsing to a point the stable leaves in each element of the Markov partition. Using the thermodynamic formalism for U, MacKay obtains an implicit expression for the Hausdorff dimension $D(\chi)$ of the subset $L(\chi)$ of the skeleton (or any smooth transversal of the stable foliation) comprised of points with positive Lyapunov exponent equal to χ.

With our representation of the dynamics as the tower over $\widetilde{T}$, which has the 2-element Markov partition $\{R_1, R_2\}$, we can derive a formula for $D(\chi)$ for any k in a simpler way. Let us consider the skeleton map $\widetilde{U}$ defined by $\widetilde{T}$, i.e., the rectangles R_1 and R_2 are collapsed into (vertical) segments I_1 and I_2, and $\widetilde{U}$ is a piecewise linear map on their union $I = I_1 \cup I_2$, with constant slope equal to $|\lambda|$, the eigenvalue of $\widetilde{M}$ (and up to a sign also of A). The lengths of the intervals $p_1 = |I_1|$, $p_2 = |I_2|$ give us the right eigenvector of $\widetilde{M}$.

We have the symbolic dynamics $\Sigma : I \to Y = \{1, 2\}^{\mathbb{N}}$ and the associated cylinder sets

$$[i_0, i_1, \ldots, i_n] = \{x \in I \,|\, \widetilde{U}^k(x) \in I_{i_k}, k = 0, 1, \ldots, n\}$$

A cylinder set is a union of segments of equal length, $|\lambda|^{-n} p_{i_n}$. Their number is equal to $\widetilde{M}(i_0, i_1) \ldots \widetilde{M}(i_{n-1}, i_n)$. Let us denote by $I^n(x)$ the unique segment of the cylinder set $[i_0, i_1, \ldots, i_n]$ which contains $x \in I$.

The positive Lyapunov exponent χ of an orbit of T is determined by the frequency f of visits to R_2 of the corresponding orbit of $\widetilde{T}$ by the formula

$$\chi = \frac{\log|\lambda|}{2f+1}. \tag{10}$$

This can be read off the schematic representation of T and $\widetilde{T}$ given in Figure 3.

Our goal is to establish the Hausdorff dimension $D(\chi)$ of the set $L(\chi)$ defined above. It follows from (10) that $D(\chi)$ is also the Hausdorff dimension of the set of points in I which under the iteration of $\widetilde{U}$ visit I_2 with frequency f.

We will give a formula for $D(\chi)$ using the classical theorem of Billingsley [B]. To that end, we construct a family of measures ξ_u, for $u \in \mathbb{R}$, as follows. Consider the positive matrices $W(u)$, $u \in \mathbb{R}$, $W(0) = \widetilde{M}$, and the Markov transition matrices $\Pi(u)$ obtained from $W(u)$ by the Parry recipe [KH],

$$W(u) = \begin{bmatrix} |k| & |k|+1 \\ e^u(|k|-1) & e^u|k| \end{bmatrix}, \quad \Pi(u) = \begin{bmatrix} \frac{|k|}{\rho(u)} & \frac{(|k|+1)p_2(u)}{\rho(u)p_1(u)} \\ \frac{e^u(|k|-1)p_1(u)}{\rho(u)p_2(u)} & \frac{e^u|k|}{\rho(u)} \end{bmatrix}. \tag{11}$$

where $\rho(u)$ is the larger eigenvalue of $W(u)$ and $(p_1(u), p_2(u))$ and $(q_1(u), q_2(u))$ are its respective right and left eigenvectors, normalized so that $\sum_i p_i q_i = 1$. In particular we have,

$$\rho^2 - (e^u+1)|k|\rho + e^u = 0, \quad e^u = \frac{\rho(\rho-|k|)}{|k|\rho - 1}, \quad \text{and} \quad \rho(0) = |\lambda|. \tag{12}$$

The transition matrices $\Pi(u)$ define ergodic Markov chains with corresponding invariant probability measures η_u on the symbolic space $Y = \{1,2\}^{\mathbb{N}}$. We want $\Sigma_* \xi_u = \eta_u$, which defines the measures ξ_u uniquely on cylinder sets. We complete the definition of ξ_u by requiring that all the intervals that constitute a cylinder set have equal measure (this construction was used previously in Section 3.4.2).

The measures ξ_u are ergodic probability measures for $\widetilde{U}$ which immediately implies

A. For ξ_u-almost-every $x \in I$ the frequency f of visits to I_2 is equal to

$$f = \xi_u(I_2) = p_2(u)q_2(u) = \frac{(\rho-|k|)(|k|\rho-1)}{|k|\rho^2 - 2\rho + |k|} = \frac{1}{2} + \frac{(e^u-1)|k|}{2\sqrt{(e^u+1)^2k^2 - 4e^u}}.$$

It follows from the form of the transition matrix $\Pi(u)$ that the measure $\xi_u(I^n(x))$ is equal up to a factor independent of n to $e^{ufn}\rho^{-n}$. Hence we get,

B. For ξ_u-almost-every $x \in I$, $\lim\limits_{n\to\infty} -\dfrac{1}{n}\log \xi_u(I^n(x)) = \log\rho(u) - fu$.

Combining B with the theorem of Billingsley [B, Theorem 14.1], we obtain,

$$D(\chi) = \lim_{n\to\infty} \frac{\log \xi_u(I^n(x))}{\log|I^n(x)|} = \frac{\log\rho(u) - fu}{\log|\lambda|}. \tag{13}$$

In light of formula (10) connecting f and χ, and using the fact that f is a monotonic function of u by item A, we obtain a formula for $D(\chi)$.

Since the explicit formula is quite cumbersome we choose to express both χ and $D(\chi)$ through ρ. Using again, (10), (12) and (13), we calculate

$$\chi D(\chi) = \frac{1}{2f+1}\log\rho - \frac{f}{2f+1}\log\frac{\rho(\rho-|k|)}{|k|\rho-1} = \log\rho - \frac{f}{2f+1}\log\frac{\rho^3(\rho-|k|)}{|k|\rho-1}.$$

From A, we also have

$$\frac{f}{2f+1} = \frac{(\rho-|k|)(|k|\rho-1)}{3|k|\rho^2 - 2(|k|^2+2)\rho + 3|k|}.$$

The evaluation of the last expression for $k=2$ gives us exactly the same function $\chi D(\chi)$ as in [M] except for the name of the variable. Our ρ is hence MacKay's parameter t.

4.4 Final remarks

Readers familiar with the thermodynamic formalism [R] will recognize that our measures ξ_u are the equilibrium states for $\widetilde{U}$ and the potential $u\log\phi$, where $\phi\equiv 1$ on I_1 and $\phi\equiv e$ on I_2. The function $\log\rho(u)$ is the topological pressure and its Legendre transform $\log\rho(u) - fu$, $f = \frac{\rho'}{\rho}$ is the metric entropy of $\widetilde{U}$ with respect to the measure ξ_u.

Indeed, using this formalism, it is possible to make explicit the connection between our potential $u\log\phi$ on I and the canonical potential $-\beta\log|U'|$ on the skeleton J where U is defined.

First define the matrix $M(\beta)$ corresponding to the potential $-\beta\log|U'|$, i.e. $M(\beta)_{i,j} = M_{i,j}|U'|^{-\beta}$. The thermodynamic formalism implies,

$$\chi D(\chi) = P(\beta) + \beta\chi, \quad \text{and} \quad P'(\beta) = -\chi, \tag{14}$$

where $e^{P(\beta)}$ is the largest eigenvalue of $M(\beta)$.

We connect the two formulas for $D(\chi)$, (13) and (14), as follows. Let ν_u be the extension of ξ_u to the skeleton $J = I_1\cup I_2\cup I_3\cup I_4$; thus $\nu_u(I_1) = \frac{1-f}{2f+1}$ and $\nu_u(I_j) = \frac{f}{2f+1}$ for $j=2,3,4$. It is immediate that ν_u is an ergodic invariant probability measure for U. We show that it is also the equilibrium state for the potential $-\beta\log|U'|$ for a specific value of β. Using (10) and (13), we write,

$$h_{\nu_u}(U) - \beta\int\log|U'|\,d\nu_u = \frac{h_{\xi_u}(\widetilde{U})}{2f+1} - \frac{\beta\log|\lambda|}{2f+1} = \frac{\log\rho(u) - fu}{2f+1} - \beta\chi = \chi D(\chi) - \beta\chi. \tag{15}$$

This last expression is equal to $P(\beta)$ for the unique β corresponding to χ via (14). This implies that ν_u is the unique equilibrium state for the potential $-\beta\log|U'|$; in other words, we could have obtained it by first applying the Parry recipe to the matrix $M(\beta)$ and then defining ν_u via the induced Markov process on 4 states, much as we did for ξ_u.

The following proposition describes the precise relations between u and β.

Proposition 4.4. *Let $t(\beta)$ be the Perron-Frobenius eigenvalue of $N(\beta) = |\lambda|^\beta M(\beta)$. Then,*

$$t(\beta) = \rho(u), \quad P(\beta) = -\frac{u}{2}, \quad t(\beta)|\lambda|^{-\beta} = e^{-\frac{u}{2}}. \tag{16}$$

Proof. We first establish that $\rho = t$. Let $\Phi = \Phi(\beta)$ be the Markov transition matrix obtained from $N(\beta)$ (equivalently $M(\beta)$) using the Parry recipe, i.e. $\Phi_{i,j} = \frac{N_{i,j} r_j}{t r_i}$ where $\vec{r}$ is the right Perron-Frobenius eigenvector of N. It is clear that $\Phi_{1,1} = |k|/t$.

The equation $N\vec{r} = t\,\vec{r}$ yields $r_1/r_4 = e^{-2P(\beta)}(|k|+1)/(t-|k|)$. Using this and the characteristic equation of N, $t^4 - |k|t^3 - (|k|t-1)|\lambda|^{2\beta} = 0$, we compute

$$\Phi_{4,1} = \frac{|k|-1}{t} \cdot \frac{r_1}{r_4} = \frac{(k^2-1)e^{-2P(\beta)}}{t(t-|k|)} = \frac{(k^2-1)|\lambda|^{2\beta}}{t^3(t-|k|)} = \frac{k^2-1}{|k|t-1}. \tag{17}$$

Since ν_u is the extension of ξ_u, the left eigenvector of Φ must be $\vec{v} = [1-f, f, f, f]/(2f+1)$. Substituting (17) into the first component of $\vec{v}\,\Phi = \vec{v}$ yields,

$$f = \frac{1-\Phi_{1,1}}{1-\Phi_{1,1}+\Phi_{4,1}} = \frac{t-|k|}{t-|k|+t\frac{k^2-1}{|k|t-1}} = \frac{(t-|k|)(|k|t-1)}{|k|t^2-2t+|k|}. \tag{18}$$

Comparing (18) with (A) proves the equivalence of ρ and t.

The second equality of (16) follows from the first by (10) and (15),

$$\log\rho(u) - fu = (2f+1)(P(\beta)+\beta\chi) = (2f+1)\Big[\log\frac{t(\beta)}{|\lambda|^\beta} + \beta\chi\Big] = \log t(\beta) + 2f\log\frac{t(\beta)}{|\lambda|^\beta},$$

which yields $-u = 2\log\frac{t(\beta)}{|\lambda|^\beta}$.

Finally, the third equality follows from the second by exponentiating both sides and noting that $e^{P(\beta)} = |\lambda|^{-\beta}t(\beta)$ by definition of $N(\beta)$. □

References

[A] R. Adler, *Symbolic dynamics and Markov partitions*, Bull. Amer. Math. Soc. **35**:1 (1998), 1-56.

[B] P. Billingsley, Ergodic Theory and Information, John Wiley and Sons: New York, 1965.

[Bo] P. Boyland, *Topological methods in surface dynamics*, Topology and Appl. **58** (1994), 223-298.

[Bu] S. Bullett, *Invariant circles for the piecewise linear standard map*, Comm. Math. Phys. **107**:2 (1986), 241-262.

[CB] A. Casson and S. Bleiler, *Automorphisms of surfaces after Nielsen and Thurston*, LMS Student Texts **9**, Cambridge University Press, Cambridge, UK, 1988.

[CG] S. Cerbelli and M. Giona, *A continuous archetype of nonuniform chaos in area-preserving dynamical systems*, J. Nonlin. Sci. **15** (2005), 387-421.

[CW] E. Cornelis and M. Wojtkowski, *A criterion for the positivity of the Lyapunov characteristic exponent*, Ergodic Theory Dynam. Systems **4**:4 (1984), 527-539.

[FR] J. Franks and E. Rykken, *Pseudo-Anosov homeomorphisms with quadratic expansion*, Proc. Amer. Math. Soc., **127**:7 (1999), 2183-2192.

[G] S. Gin, *Large deviations rate function for the distribution of finite-time shear rotation rates of $\mathcal{H}$*, Master's Thesis, University of Warwick (2006).

[KH] A. Katok and B. Hasselblatt, *Introduction to the Modern Theory of Dynamical Systems*, Cambridge University Press, Cambridge, UK, 1995.

[LW] C. Liverani and M. Wojtkowski, *Ergodicity in Hamiltonian systems*, Dynamics reported, pp 130-202, Dynam. Report. Expositions Dynam. Systems (N.S.), 4, Springer, Berlin, 1995.

[M] R. MacKay, *Cerbelli and Giona's map is pseudo-Anosov and 9 consequences*, J. Nonlin. Sci. **16** (2006), 415-434.

[R] D. Ruelle, *Thermodynamic formalism*, second ed., Cambridge University Press: Cambridge, UK, 2004.

[T] W.P. Thurston, *On the geometry and dynamics of diffeomorphisms of surfaces*, Bull. Amer. Math. Soc. **19** (1988), 417-431.

[W1] M. Wojtkowski, *A model problem with the coexistence of stochastic and integrable behaviour*, Comm. Math. Phys. **80**:4 (1981), 453-464.

[W2] M. Wojtkowski, *On the ergodic properties of piecewise linear perturbations of the twist map*, Ergodic Theory Dynam. Systems **2**:3-4 (1982), 525-542